

Morphology of PPGI signals upon stimulation

Sebastian Zaunseder, Vincent Fleischhauer

Angaben zur Veröffentlichung / Publication details:

Zaunseder, Sebastian, and Vincent Fleischhauer. 2024. "Morphology of PPGI signals upon stimulation." In 2024 Computing in Cardiology Conference (CinC), September 8-11, 2024, Karlsruhe, Germany, 1-4. Computing in Cardiology (CinC). <https://doi.org/10.22489/cinc.2024.203>.

Morphology of PPGI Signals upon Stimulation

Sebastian Zaunseder¹, Vincent Fleischhauer²

¹ University of Augsburg, Augsburg, Germany

² Dortmund University of Applied Sciences and Arts, Dortmund, Germany

Abstract

Photoplethysmography imaging (PPGI) can yield far-reaching statements on the health state in a convenient way. The presented work investigates the morphology of PPGI signals upon stimulation in comparison to the behavior of contact PPG signals. We use own experimental data of 39 healthy volunteers recorded during a cold pressure test (CPT). We analyze PPGI signals from the face and from the forearm together with contact PPG from the finger and the earlobe. Signals' morphology is assessed by means of four common features at three time intervals around CPT. Our results show significant differences upon stimulation for most features from finger and earlobe PPG ($p < 0.001$). Even PPGI signals show significant differences upon stimulation, though forearm signals' analysis is hampered by a lower signal quality. Beyond a general effect of stimulation, there are differences in the signals' behavior according to the recording setup. E.g., finger and forearm signals show stronger and even more persistent effects upon stimulation than earlobe and facial signals. Our study highlights the importance of recording setup. While care must be taken when knowledge or methods are transferred from contact PPG to PPGI, the found behavior opens novel analysis opportunities if multiple PPG signals are available.

1. Introduction

Over the last years, photoplethysmography imaging (PPGI) has attracted immense attention. PPGI assesses the cutaneous perfusion by exploiting subtle color variations from videos to yield variable (patho)physiological information. PPGI can capture multiple parameters such as heart rate (HR), heart rate variability (HRV), oxygen saturation, blood pressure and strength of cutaneous perfusion [1–3]. Such variety, together with its ease-of-use and economic factors, make PPGI extremely attractive and open up multiple clinical and non-clinical applications [2, 4].

Despite remarkable progress, PPGI is still in its early stages. Besides limited evidence from real-world applica-

tions, there is a lack of fundamental knowledge on the origin of PPGI, signals' behavior and derivable statements. Accordingly, more basic research is required towards developing tailored processing methods and exploiting the full potential of PPGI.

The presented work is dedicated to such basic research. In an earlier work, we analysed the behavior of facial PPGI versus contact PPG showing distinct differences [5]. Within this work, we extend our previous considerations by including PPGI from the forearm.

2. Material and Methods

2.1. Data

Our contribution employs data from own multimodal experiments invoking healthy volunteers of Caucasian origin. Following we provide a short summary on those aspects, which are relevant for the current contribution. A more detailed description of the study protocol, equipment and participants is contained in [5].

Experimental protocol: The experiments were carried out on a tilt table and covered different stimuli. Within this work, only the cold pressure test (CPT) is analysed. CPT is known to provoke a strong physiological reaction, mostly an increase in blood pressure. During CPT, participants placed their left hand in supine position into cold water of approx. 4 °C for 60 s (participants could quit earlier if necessary). Our analysis used three time intervals of 10 s in relation to the time of immersion t_{CPT} : baseline (BL), starting at $t_{\text{CPT}} - 30$ s, stimulation 1 (ST1), starting at $t_{\text{CPT}} + 20$ s and stimulation 2 (ST2), starting at $t_{\text{CPT}} + 40$ s. Figure 1 shows the relevant part of the experiment protocol and placing of the analysis intervals.

Data acquisition: PPG signals were recorded from right earlobe and right index finger by two biosignal amplifiers Biopac MP36 (Biopac; Goleta, United States of America) and reflective photoplethysmographic signal transducers SS4LA (Biopac; Goleta, United States of America) (sampling rate of 2000 Hz, emitter/detector wavelength of 860 ± 60 nm). Videos from the face and the forearm were recorded by UI-3060CP-C-HR Rev

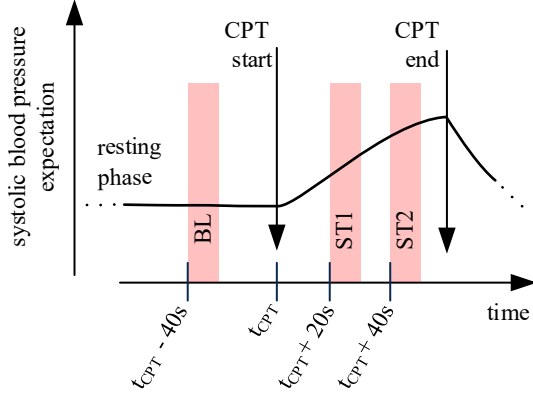


Figure 1: Expected reaction of systolic blood pressure upon CPT and placement of used analysis intervals before stimulation (baseline, BL) and after stimulation (ST1, ST2). The timing was chosen to capture the effect of CPT but exclude phases, which are likely to be affected by movement artifacts.

2 RGB cameras (IDS Imaging Development Systems GmbH; Obersulm, Germany). The cameras were mounted on the tilt table and had fixed orientation regarding the subject during the experiment. Videos from the face were captured at a color depth of 12 bit, a frame rate of 25 Hz and a spatial resolution of 1280×960 pixel. The camera for the forearm used a frame rate of 200 Hz and a spatial resolution of 640×480 pixel. We used indirect artificial illumination by two spotlights Walimex pro LED Sirius 160 Daylight 65W (color temperature 5600 K, color rendering index ≥ 90) (WALSER GmbH & Co. KG; Gersthofen, Germany).

Participants: Overall, 61 recordings were carried out. For technical reasons or early stopping the experiment not all of them are usable. We finally include 39 recordings in our analysis (13 female, 26 male; age: 30.5 ± 12.0 years; body height: 177 ± 7.83 cm; body weight: 76.5 ± 14.9 kg).

2.2. Signal processing

The processing of photoplethysmographic signals (PPGI and PPG) relates to the methods described earlier [5, 6] and was applied to all intervals of 10 s. In short, for PPGI we first manually defined regions of interest (ROI) in the face and on the forearm using proprietary software (see Figure 2 for two examples). From such ROIs, we derived PPGI signals per color channel by averaging. Note that the further statements and quantitative analyses use the green channel but we will refer to the red channel qualitatively. The further processing is the same for PPGI and PPG signals. Thereby, each signal is handled separately. We filtered the signals with a bandpass filter (5th-order Butterworth filter with cut-off frequencies



(a) Facial ROI consisting of the forehead and both cheeks. (b) Forearm ROI at the bottom of forearm spanning its width

Figure 2: Illustration of ROIs from face and forearm (blue colored parts)

of 0.4 Hz and 8 Hz). Single beats from all signals were detected using the method of Lazaro et al. [7]. All detected beat segments were correlated pairwise and those with a mean pairwise correlation lower than 0.3 were discarded. For the remaining beats, we removed linear trends and applied ensemble averaging to form a beat template for each interval of 10 s. Finally, we derived four commonly used features from the denoised templates, namely amplitude (maximum of the template), slope (maximum of the first derivative of the template), area (area under the template) and PWHA (pulse width at half amplitude).

2.3. Statistical assessment

The statistical assessment applies to each of the aforementioned features and compares the intervals BL, ST1 and ST2. Again, each modality (PPGI and PPG) and wavelength was considered separately. We firstly conducted repeated measures ANOVA on a significance level of $\alpha = 0.05$. If ANOVA yielded significant difference, we conducted paired t-tests ($\alpha = 0.05$) as post-hoc tests between intervals and used Holm-Bonferroni correction to adjust the p values of our post-hoc tests. As a measure of effect size we calculated Hedges' g . Effect sizes $|g| < 0.5$ are considered small, while $|g| > 0.8$ are considered large.

3. Results

We had to exclude four subjects from the analysis as no beat template could be generated in at least one of the analysis intervals. Thus, the results base on data from 35 subjects. Figure 3 shows a representative set of templates from PPG and PPGI as an example. Figure 4 shows exemplary results for the contact PPG and PPGI from face and forearm. Table 1 contains further numerical results.

4. Discussion

General observations: As illustrated in Figure 3, templates typically show morphological differences according to the modality, with a tendency of contact PPG templates

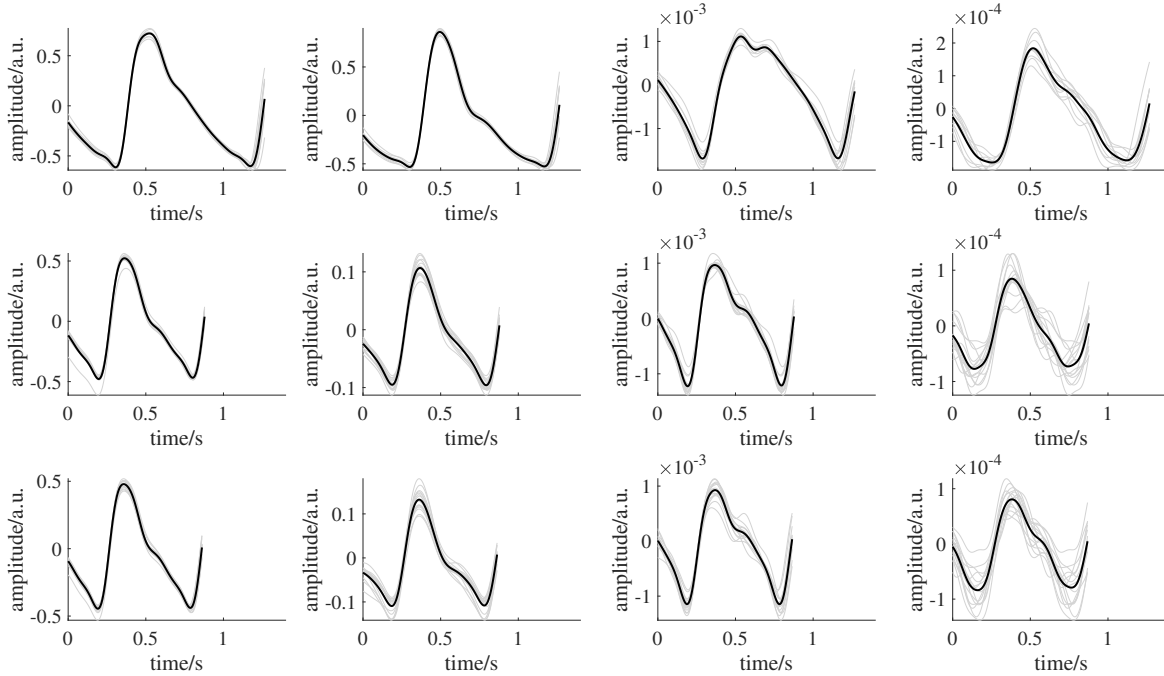


Figure 3: Exemplary templates of one subject. From left to right: earlobe PPG, finger PPG, facial PPGI (green channel) and forearm PPGI (green channel). The upper row shows signals during BL. The middle row shows signals during ST1. The lower row shows signals during ST2. Black lines indicate mean beat templates; gray lines indicate the corresponding beat segments.

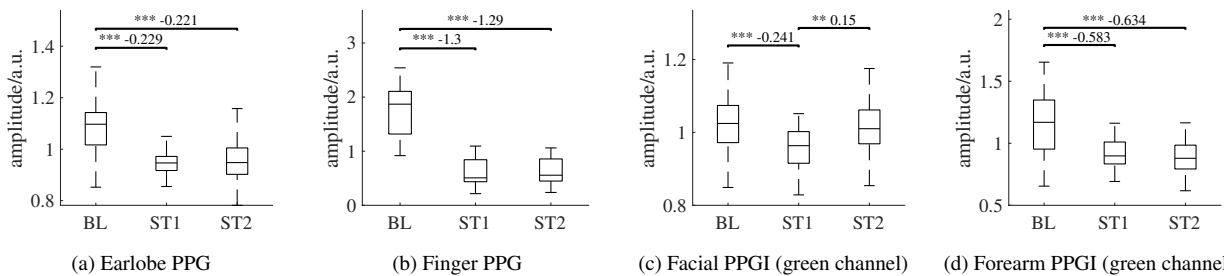


Figure 4: Behavior of the beat amplitude for the different modalities together with results of post-hoc testing (* for $p < 0.05$, ** for $p < 0.01$ and *** for $p < 0.001$) and effect sizes where post-hoc tests yielded significant differences.

to decay earlier. Such behavior might be related to the fact that in PPGI, particularly considering the green channel, more superficial vessels with greater capacity to pool blood contribute to signals' generation. As expected, the forearm signals shows lower signal quality and larger variations between single beats. Similar, other color channels (see figure 5) show reduced signal quality.

Effect of CPT: CPT has an effect on photoplethysmographic signals in all setups. According to Hedge's g , effects at the extremity (PPG and PPGI) are, on average, more pronounced than at the face. While at the extremity, PPG shows stronger effects than PPGI, differences vanish at the face. Further, as we reported earlier [5, 8], fa-

cial PPGI signals' morphology tends to recover faster after CPT than PPG (positive g when comparing ST1 and ST2). Forearm PPGI, in turn, does not show this tendency underlining the more pronounced effect of measurement site as compared to the recording setup. We attribute the found behavior to a combination of four factors: first, the face is less affected by vasoconstriction compared to the extremities. Second, signal contributing vessels in PPGI are less affected by vasoconstriction. Third, lacking contact pressure allows vessels to recover quicker. Fourth, signals' instability in PPGI contributes to reduced effect sizes. For the red channel, we observed a similar behavior as for the green channel. Thus, measurement site has more influence

Table 1: Results for PPG and PPGI’s green channel. Shown are effect sizes between intervals. Colored cells show effect sizes for statistically significant differences.

Measurement	BL - ST1	BL - ST2	ST1 - ST2
PWHA			
PPGI face	-0.48	-0.46	0.02
PPGI forearm	-0.27	-0.22	0.06
PPG finger	0.61	0.73	0.11
PPG ear	-0.30	-0.29	0.01
amplitude			
PPGI face	-0.24	-0.10	0.15
PPGI forearm	-0.58	-0.63	-0.06
PPG finger	-1.30	-1.29	0.02
PPG ear	-0.23	-0.22	0.01
area			
PPGI face	-0.40	-0.25	0.15
PPGI forearm	-0.59	-0.67	-0.06
PPG finger	-1.19	-1.17	0.06
PPG ear	-0.35	-0.33	0.02
slope			
PPGI face	-0.26	-0.32	-0.04
PPGI forearm	-0.52	-0.58	-0.04
PPG finger	-1.33	-1.35	-0.05
PPG ear	-0.26	-0.37	-0.11

than such wavelength differences. However, as Figure 5 shows, the signal quality is markedly worse. This made the exclusion of further subjects necessary which is why we avoid providing quantitative results.

5. Conclusion

PPGI can capture effects of distal stimuli at multiple measurement sites. Owing to physiological reasons, there are differences between facial and forearm PPGI. In addition, owing to lower penetration depths at visible wavelengths and missing contact pressure PPGI signals are less affected by stimuli and recover faster than PPG signals. Overall, our findings highlight the importance to consider physiological mechanisms when designing algorithms and trying to transfer knowledge from contact PPG to PPGI.

Acknowledgments

This work was funded by the German Research Foundation (DFG), project 401786308.

References

[1] Chen W, Yi Z, Lim LJR, Lim RQR, Zhang A, Qian Z, Huang J, He J, Liu B. Deep learning and remote photoplethysmography powered advancements in contactless physiologi-

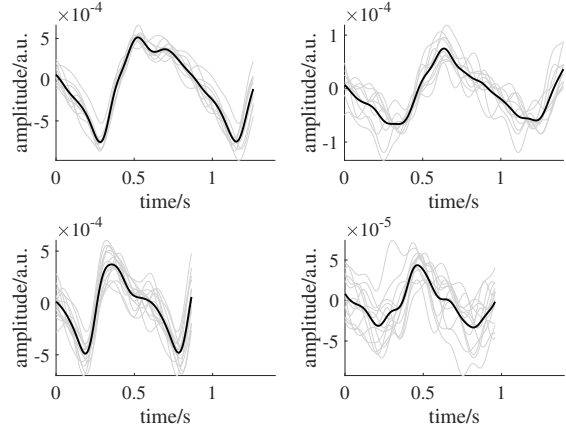


Figure 5: Exemplary PPGI templates (black line; single beats gray lines) using the red channel (left face, right forearm; upper row BL, lower ST2).

cal measurement. *Frontiers in Bioengineering and Biotechnology* 2024;12(July). ISSN 22964185.

[2] Molinaro N, Schena E, Silvestri S, Bonotti F, Aguzzi D, Viola E, Buccolini F, Massaroni C. Contactless Vital Signs Monitoring From Videos Recorded With Digital Cameras: An Overview. *Frontiers in Physiology* 2022;13(February).

[3] Zaunseder S, Trumpp A, Wedekind D, Malberg H. Cardiovascular assessment by imaging photoplethysmography – a review. *Biomedical Engineering Biomedizinische Technik* oct 2018;63(5):617–634. ISSN 1862-278X.

[4] Zaunseder S, Rasche S. Clinical applications for imaging photoplethysmography. In *Contactless Vital Signs Monitoring*. Elsevier, 2022; 149–164.

[5] Fleischhauer V, Bruhn J, Rasche S, Zaunseder S. Photoplethysmography upon cold stress—impact of measurement site and acquisition mode. *Frontiers in Physiology* jun 2023; 14(June):1–15. ISSN 1664-042X.

[6] Fleischhauer V, Ruprecht N, Sorelli M, Bocchi L, Zaunseder S. Pulse decomposition analysis in photoplethysmography imaging. *Physiological Measurement* oct 2020; 41(9):095009. ISSN 1361-6579.

[7] Lázaro J, Gil E, Vergara JM, Laguna P. Pulse rate variability analysis for discrimination of sleep-apnea-related decreases in the amplitude fluctuations of pulse photoplethysmographic signal in children. *IEEE Journal of Biomedical and Health Informatics* 2014;18(1):240–246.

[8] Fleischhauer V, Woyczyk A, Rasche S, Zaunseder S. Impact of sympathetic activation in imaging photoplethysmography. In *2019 IEEE/CVF International Conference on Computer Vision Workshop (ICCVW)*. IEEE. ISBN 978-1-7281-5023-9, oct 2019; 1697–1705.

Address for correspondence:

Prof. Dr.-Ing. Sebastian Zaunseder
Eichleitnerstr. 30, 86159 Augsburg, Germany
sebastian.zaunseder@uni-a.de